Autoxidation of Siphonochilone in processed rhizomes and stored powders of *Siphonochilus aethiopicus* (Schweinf.) B.L. Burtt

Félix Katele Zongwe,[a] Jules Tshishimbi Muya[b,c], Raphael Mutimana[b], Mudogo Virima[b], Muzomwe Mayaliwa[b], Hoeil Chung[c] and Vinesh Maharaj*[a]

Abstract: A furano sesquiterpenoid, known as siphonochilone (**1**), is commonly reported as the major compound in the roots and the rhizomes of *Siphonochilus aethiopicus* together with related oxidized sesquiterpenoids (**2**-**5**). As part of investigating the UPLC QTOF MS ES+ chemical profiles of n-hexane/dichloromethane (1:1) extracts from crushed fresh rhizomes, dried and powdered rhizomes and the dried powders held under storage at room temperature, we have recently realized that decomposition of **1** occurs during the processing of the rhizomes and the storage of the powders. This decomposition which involves autoxidation of the furan moiety leads to formation of the artefact sesquiterpenoid lactone (**3**) and potentially (**4**), which numerous papers misreport as naturally present in the plant. MP2/6-31+G(d,p), B3LYP/6-31+G(d,p) and B3LYP/6-311+G(2d,p) calculations were performed on siphonochilone (**1**) and the sesquiterpenoid lactone artifacts (**3**) and (**4**) and results rationalized the observed autoxidation.

Keywords: African ginger • siphonochilus aethiopicus• siphonochilone • autoxidation

[a] F. Z. Katele, Prof. V. Maharaj
Department of Chemistry
University of Pretoria
Lynnwood road, Private Bag X20, Pretoria 0002 (South Africa)
E-mail: vinesh.maharaj@up.ac.za

[b] Prof. J. T. Muya, R. Mutimana, Prof. M. Virima, Prof. M. Mayaliwa,
Department of Chemistry
Faculty of Science, University of Kinshasa, P.O.Box 190 Kinshasa XI, DR Congo

[c] Prof. J.T. Muya, Prof. Hoeil Chung
Department of Chemistry
Faculty of Natural Science, Hanyang University, Seoul, Korea
E-mail: hoeil@hanyang.ac.kr

Supporting information for this article is given via a link at the end of the document.

Introduction

Siphonochilus aethiopicus (Schweinf.) B.L. Burtt, also known as African ginger, is a deciduous rhizomatous species in the Zingiberaceae family and indigenous to savanna regions of tropical and southern Africa.[1-3] The rhizomes of the plant are highly prized in the South African traditional medicine for its health benefits where it is widely employed as a local remedy against a number of ailments such as asthma, colds, coughs, hysteria and influenza.[4-8] In 2002, two furano sesquiterpenoids, viz. siphonochilone (**1**) and its hydroxylated derivative (**2**), and their relative configurations were reported by Holzapfel et al.[3] after steam distillation of fleshy crushed roots while three aditional sesquiterpenoid lactones (**3**-**5**) were purified and reported in 2009 from an ethylacetate extract of dried and powdered rhizomes by Lategan et al.[5] The relative structures are shown in Figure 1.

In our studies we aimed at investigating the chemical profiles using ultra performance liquid chromatography coupled to mass spectrometry (UPLC QTOF MS ES+) of n-hexane/dichloromethane (1:1) extracts prepared from crushed fresh rhizomes, processed and powdered rhizomes and powders stored under room temperature conditions for nine months. We have observed that levels of siphonochilone (**1**) reduce through oxidation of its furan moiety upon storage, leading to formation of more stable sesquiterpenoid lactones (**3**) and (**4**).

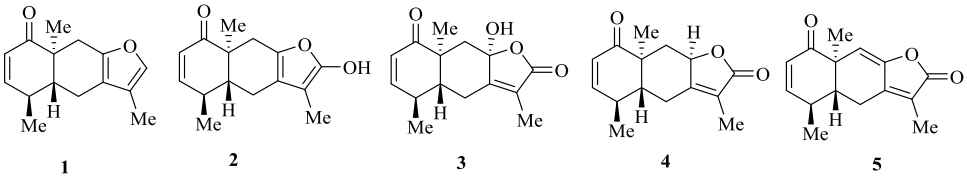

Figure 1. Siphochilone (**1**), its hydroxylated derivative (**2**) and related sesquiterpernoid lactones (**3-5**).

Results and Discussion

Autoxidation of siphonochilone after plant processing and storage of the powder

Dried n-hexane/dichloromethane (1:1) extracts from crushed fresh rhizomes, freshly processed and powdered rhizomes and from powders stored for nine months at room temperature were subjected to UPLC QTOF MS analyses using positive electrospray ionization (ES+). Results of the extract from the fresh rhizomes are expressed as chromatographic chemical profiles of the secondary metabolites and four characteristic peaks, labeled A-D, were annotated (Figure 2a). The most intense peak D was identified as siphonochilone **1** after purification – as a colorless crystalline compound (Figure 2b), and molecular characterization through MS, NMR, IR, X-ray diffraction experiments (XRD), and B3LYP/6-311+G(2d,p)[9] structure optimization.

QTOF MS ES+ data from the UPLC elution of the isolated siphonochilone **1** displayed a $[M+H]^+$ molecular ion with m/z 231.1387 (Figure 2b) which corresponded to the molecular formula $C_{15}H_{18}O_2$. Intensive NMR investigations established the relative configuration of **1**, which latter corroborated the XRD structure (Figure 3a) as well the B3LYP/6-311+G(2d,p) optimized geometry (Figure 3b).

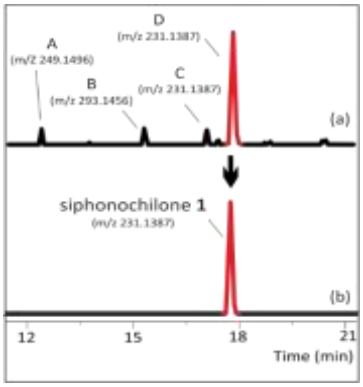

Figure 2. (a) UPLC QTOF MS ES+ chemical profile of the extract prepared from fresh rhizomes (b) UPLC QTOF MS ES+ chromatogram of the isolated siphonochilone **1.**

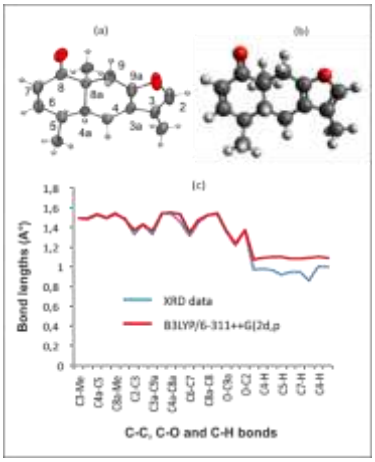

Figure 3. (a) X-ray crystallography structure (b) B3LYP/6-311++G(2d,p) optimized geometry of siphonochilone **1 (c)** Comparison between bond distances of the B3LYP/6-311++G(2d,p) optimized geometry (red curve) and X-ray geometrical data (blue curve) of siphonochilone **1.**

Comparison between XRD structural data and B3LYP/6-311+G(2d,p) geometrical parameters validated the identity of siphonochilone **1**. The computed bond distances matched perfectly with experimental data (Figure 3c). Small deviations were however observed for C-H bonds. This shortening of bonds in the experimental XRD geometry commonly arises from the arrangement of molecules within the crystalline solid.(10) This may also be a result of incorrectly defined proton positions in the XRD experiment – an often encountered effect.

Tables 1 and 2 compare the NMR experimental data with the results derived from B3LYP/6-311+G(2d,p) quantum chemical calculations in dichloromethane.

The similarity between the experimental and theoretical ^{13}C and ^{1}H NMR chemical shifts relative to TMS as well as the ^{1}H spin–spin coupling (Table 1 and 2) constants undoubtedly proved the isolated compound to be siphonochilone (**1**)**.**

Further validation of the molecular structure of siphonochilone arose from the matching of theoretical and experimental vibrational frequencies, which were found to be in good agreement despite minor shifts (Table 3). These shifts in frequencies give a glimpse on the strength of the intermolecular interactions in the crystalline solid of siphonochilone **(1)** and show the effect of the media in the solid state IR, referring to the fact that the theoretical IR spectrum was achieved in gas phase. It is known that C-C bonds are more rigid and constitute the backbone of the molecular system on which other pendant functions such as C-H are linked. The pendant

groups are more flexible and can be involved in intermolecular interaction with neighbouring molecules in condensed phase, hence causing vibrational frequencies shifts.[10]

The three other peaks marked as A, B and C (Figure 2a) could not unambiguously be related to any of the sesquiterpenoids reported from African ginger and shown in Figure 1.

Table 1. NMR Spectroscopic Data (400 MHz, CD_2Cl_2) for siphonochilone (**1**). Labels refer to the X-ray structure of **1** in Figure 3a. B3LYP/6-311+G(2d,p) chemical shifts relative to TMS in dichloromethane are shown in parenthesis.

Position	δ_C , type	δ_H	HMBC
2	137.8 (142.6), CH	7.1, *m* (7.3)	
3	119.7 (128.2),C		
3a	115.3 (121.4),C		
4	22.8 (25.6), CH_2	2.7, *ddd* (2.8) 2.1, *dddd* (2.2)	3a, 4a, 9a 3-Me
4a	45.3 (49.7), CH	1.9, *ddd* (1.8)	4, 5, 8a, 8a-Me
5	34.6 (39.4), CH	2.4, *m* (2.6)	
6	154.8 (166.3), CH	6.7, *dd* (7.2)	4a, 5, 8, 5-Me
7	126.7 (131.1), CH	5.9, *dd* (6.1)	5
8	204.2 (214.5), C		
8a	45.3 (50.9), C		
9	32.3 (34.7), CH_2	2.7, *dd* (2.7) 2.6, *br d* (2.6)	3a, 4a, 9a, 8a-Me 9a, 8a-Me
9a	149.6 (157.7),C		
3-Me	8.2 (8.8), CH_3	1.9, *d* (1.9)	2, 3, 3a
5-Me	18.9 (18.9), CH_3	1.2, *d* (1.3)	4a, 5, 6
8a-Me	16.8 (17.3), CH_3	1.0, *s* (1.1)	4a, 8, 9

Table 2. Experimental 1H-1H spin spin coupling constants (400 MHz, CD_2Cl_2) for siphonochilone (**1**) and that computed at B3LYP/6-311+G(2d, p) in dichloromethane.

Position	Type	Exp.(Hz)	B3LYP/6-311+G(3d, 2p)
4	CH_2	(15.9, 5.4, 1.8)	(15.5, 5.4, 2.0)
		(15.9, 11.0, 3.1, 1.7)	(15.5,9.4,3.5,1.6)
4a	CH	(10.9, 9.9, 5.4)	(9.4, 8.0, 5.4)
6	CH	(10.1, 2.2)	(9.4, 2.4)
7	CH	(10.1, 2.8)	(9.4, 3.4)
9	CH_2	(16.8, 1.7)	(16.7, 1.9)
		(16.8)	(16.7, 1.6)
3-Me	CH_3	(1.3)	(2.2)
5-Me	CH_3	(7.2)	(11.7)
8a-Me	CH_3		

Table 3. Assignment of different stretching vibrational modes of **1** computed at B3LYP/6-311+G(2d,p) *in vacuo* and that carried out experimentally in the solid state.

Experimental frequency	Theoretical frequency	shifts	Assignments	Intensities
3131-3019	3261-3136	44-130	ν C-H	av,w
2968	3109-3087	119-141	νCH_3	s
2932-2849	3071-3051	139-202	ν C H_2	s
1759	1698	61	νC =O	s
1673-1646	1677-1589	4-57	νC=C	av,w

Investigation of the n-hexane/dichloromethane (1:1) extract prepared from the powder obtained right after processing the sliced, dried and grinded rhizomes displayed a chemical profile (Figure 4b) similar to that from the fresh plants (Figure 4a), with siphonochilone being the major peak. However, an additional minor peak could be detected in the profile from the processed plants at 10.03 min (m/z 245.1180), see the purple peak in the zoomed region in Figure 4b. This peak was observed to intensify in the chromatogram of the extract prepared from the stored powder (see the purple peak in Figure 4c). The latter chromatogram revealed three characteristic peaks while lacking a peak corresponding to siphonochilone. Of these three peaks, two labelled E and F were newly formed, as they were completely absent in the chromatogram of the fresh rhizomes (Figure 4a). The compound which corresponds to peak E was unambiguously identified after isolation, crystallization and structure elucidation as the sesquiterpenoid lactone **3**.

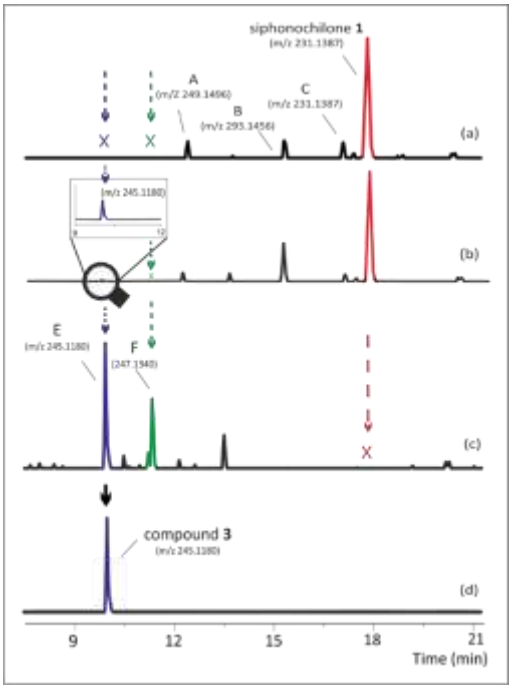

Figure 4. UPLC MS ES+ chemical profiles of extracts from (a) fresh rhizomes, (b) processed plants, (c) stored powder (d) chromatograms of the pure compound **3**.

UPLC QTOF MS ES+ analysis of the isolated compound **3** showed a single peak (Figure 4d) with a $[M+H]^+$ corresponding to *m/z* 263.1282 and an abundant base peak of *m/z* 245.1180 $[M+H-H_2O]^+$. The $[M+H]^+$ molecular ion (*m/z* 263.1282) was assigned the formula $C_{15}H_{18}O_4$.

The relative molecular structure was derived from NMR analyses, XRD experiments and B3LYP/6-311+G(3d,2p) theoretical calculations. Tables 4 and 5 provide B3LYP/6-311+G(2d,p) data of ^{13}C and ^{1}H NMR chemical shifts relative to TMS as well as the ^{1}H spin–spin coupling in chloroform.

Table 4. NMR Spectroscopic Data (400 MHz, CD_3Cl) for compound **3**. Labels refer to the X-ray structure of **3** in Figure 5a. B3LYP/6-311+G(2d,p) chemical shifts relative to TMS in chloroform are shown in parenthesis.

Position	δ_C , type	δ_H	HMBC
2	172.1 (178.4), C		
3	122.4 (130.0), C		
3a	158.5 (169.7),C		
4	24.1 (27.0), CH_2	2.8, *dd* (2.9) 2.4, *m* (2.4)	3, 4a, 8a, 9a 3-Me
4a	49.9 (55.6), CH	1.6, *ddd* (1.5)	8a-Me
5	33.8 (39.2), CH	2.5, *dqt* (2.6)	
6	153.6 (164.2), CH	6.6, *dd* (7.1)	4a, 5, 8, 5-Me
7	126.1 (131.3), CH	5.9, *dd* (6.0)	5
8	202.9 (212.6), C		
8a	44.9 (51.2), C		

9	43.7 (46.2), CH_2	2.6, *d* (2.7) 1.7, *d* (1.5)	3a, 4a, 9a, 8a, 9a 9a, 8a, 8a-Me
9a	103.5 (110.0), C		
9a-OH		4.1, *s* (1.4)	
3-Me	8.2 (9.1), CH_3	1.8, *d* (1.8)	2, 3, 3a
5-Me	18.1 (18.5), CH_3	1.2, *d* (1.3)	4a, 5, 6
8a-Me	16.7 (17.6), CH_3	1.3, *s* (1.4)	4a, 8, 8a

Table 5. Experimental 1H-1H spin spin coupling constants (400 MHz, CD_3Cl) for compound **3** and that computed at B3LYP/6-311+G(2d, p) in chloroform.

Position	Type	Exp.(Hz)	B3LYP/6-311+G(3d, 2p)
4	CH_2	(13.5, 3.6)	(12.9, 3.4) (12.9, 11.0, 2.7)
4a	CH	(13.3, 10.0, 3.6)	(11.0, 3.4, 3.0)
6	CH	(10.1, 2.0)	(9.4, 3.4)
7	CH	(10.1, 2.7)	(9.4, 3.4)
9	CH_2	(14.5) (14.5)	(14.1) (14.1)
3-Me	CH_3	(1.4)	(2.7)
5-Me	CH_3	(7.1)	(11.6)
8a-Me	CH_3		

Comparison between structural data from XRD and the molecular parameters issued from B3LYP/6-311+G(2d,p) calculations for the sesquiterpenoid lactone **3** showed a good match between experimental and predicted bond lengths with small deviations for C-H and O-H distances (Figure 5c). The observed deviations could be explained as a result of O-H…O intramolecular hydrogen bond (IHB) formation in the crystal structure, between the hydroxyl group and its neighboring oxygen atom of the five-membered ring. Both B3LYP/6-31+G(d,p) and MP2/6-31+G(d,p)[9b,11] showed this intramolecular O-H…O bond to provide a small stabilization energy of 0.13 kcal/mol and 0.16 kcal/mol, respectively, compared to the geometric structure optimized without consideration of the O-H…O IHB.

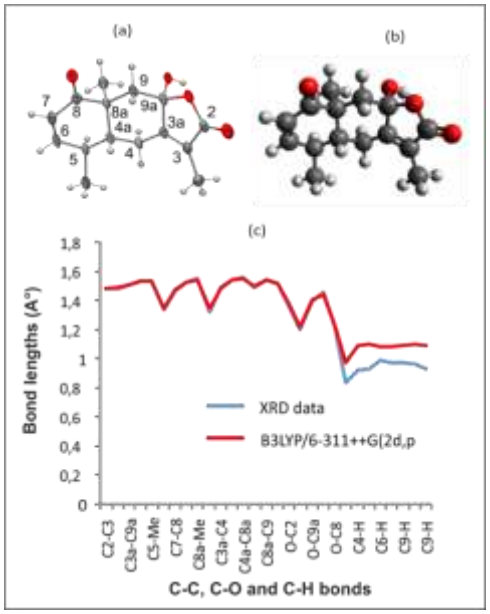

Figure 5. (a) XRD crystallographic structure of **3** (b) B3LYP/6-311++G(2d,p) optimized geometry (c)**.** Comparison between the bond distances of the B3LYP/6-311++G(2d,p) optimized geometry (red) and X-ray geometry (blue) of sesquiterpenoid lactone **3.**

Good correlation was also observed between the solid state experimental IR data and the B3LYP/6-311+G(2d,p) harmonic frequencies (Table 6). The shifts in frequencies could be depicted as a result of intra and intermolecular interactions arising within the solid crystal of the sesquiterpenoid lactone **3**. C-H, O-H, and C=O groups can in fact interact with neighbouring molecules through intermolecular hydrogen bonds. The largest redshifts observed for O-H and C-H was in good agreement with the bond lengths difference displayed in Figure 5c.

The peak labeled F (Figure 4c) showed a molecular ion $[M+H]^+$ with m/z 247.1338 which corresponded the molecular formula $C_{15}H_{18}O_3$. This formula matched those of the sesquiterpenoids (**2**) and (**4**). After isolation and characterization of its molecular structure, the peak F was conclusively identified as compound **4**. This was done through comparison of the acquired NMR data with the ^1H and ^{13}C chemical shifts reported in the literature (see supporting information) as well as the data predicted at the B3LYP/6-311+G(2d,p) theoretical level**.** These results reliably indicated that the two sesquiterpenoid lactones **3** and **4** originated from the autoxidation of siphonochilone (**1**) and are formed during storage of the dry powder.

Table 6. Assignment of different stretching vibrational modes of **3** computed at B3LYP/6-311+G(2d,p) *in vacuo* and that carried out experimentally in the solid state.

Experimental frequencies	Theoretical frequencies	shifts	Assignments	Intensities
3425	3794	369	ν O-H	s
3131-3019	3197-3150	44-117	ν C-H	av,w
2968	3152-3125	93	νCH_3	s
2932-2849	3078-3017	119-168	ν CH_2	s
1759-1673	1836-1747	77-74	νC =O	vs
1646	1743-1681	4-57	νC=C	av,w

Autoxidation of the purified siphonochilone

To rationalize the conversion of siphonochilone **1** into the more oxidized sesquiterpenoid lactones **3** and **4** during storage, UPLC QTOF MS ES+ investigation was conducted on the isolated and stored siphonochilone. The crystals was stored in transparent glass vials at room temperature and visually monitored on a regular basis for 5 months. The initially colorless crystals were gradually observed to turn brownish on standing. UPLC QTOF MS ES+ investigation of the brownish crystals showed two additional peaks, in addition to that of siphonochilone **1** (Figure 6b). Comparison between the generated chromatographic data with the chemical profile of the extract prepared from the powder held under storage (Figure 6c) showed that the two new peaks – labeled E' and F', to be the same as those observed for the stored powder (Figure 6b versus Figure 6c), giving that retention times as well as MS data were in perfect agreement. From this matching, the identity of E' was thus reliably confirmed to be the hydroxy lactone derivative **3**, while that of F' was established to be **4** (supplementary information).

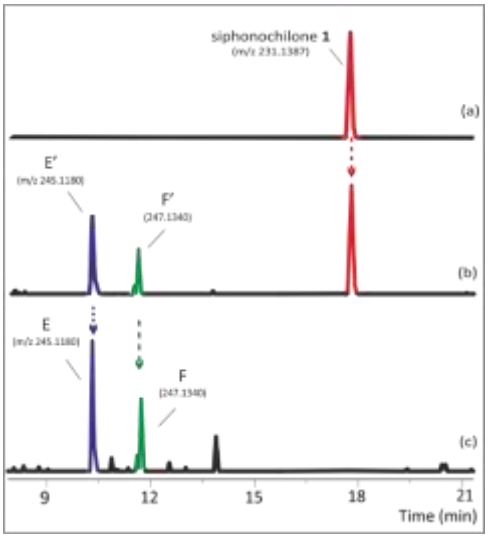

Figure 6. UPLC MS ES+ chromatogram of siphonochilone (a), siphonochilone after autoxidation (b) and stored powder (c).

The above results clearly indicated that autoxidation of siphonochilone occurs in the stored powder as well as in the isolated crystals held in the glass transparent vial, leading to formation of more oxidized artefacts, such as the lactones **3** and **4**.

Rationalization of the autoxidation of siphonochilone **1** into the more oxidized artefacts was achieved through an intensive study of HOMO and LUMO orbitals of compounds **1-4**. Computations were carried out at MP2/6-31+G(d,p) level and results are portrayed in Figure 7 for compounds **1**-**4**. Results estimated the HOMO-LUMO gap energy of **2** to be about 9.35 eV, that of **3** as 11.60 eV, while that of **4** was found to be approximately 11.29 eV. Comparison between the HOMO-LUMO gap energies of the compounds **3** and **4** with that of siphonochilone **1** which was established as 9.66 eV, revealed the more oxidized compounds **3** and **4** as more kinetically stable entities, given their greater HOMO-LUMO gaps while that for compound **2** is close to that of **1**. These results might justify the observed autoxidation of Siphonochilone **1** to form chemically more stable artefacts such as **3** and **4,** fact being that the difference between the HOMO-LUMO gap potential energies is a driving force of different types of chemical reactions.

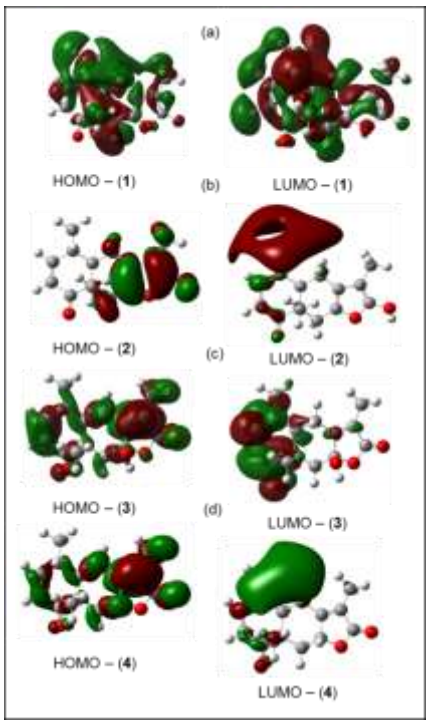

Figure 7. Frontier molecular orbitals of siphonochilone **1** and its structurally related sesquiterpenoids **2**-**4**.

Conclusions

A furano sesquiterpenoid, known as siphonochilone **1**, is commonly reported as the major compound in the roots and the rhizomes of African ginger together with closely related sesquiterpenoid derivatives (**2**-**5**). We demontrasted in this study that autoxidation of siphonochlone **1** occurs during the processing of the rhizomes and the storage of the powders, leading to formation of artifact lactone derivatives **3** and **4** which numerous papers might be misreporting as naturally present in the African ginger rhizomes. MP2/6-31+G(d,p) theoretical investigation of the frontier molecular orbitals as well as the HOMO-LUMO potential energy gaps proved the artefact **3** and **4** to be more chemically stable than **1**, hence justifying autoxidation of Siphonochilone **1** into more stable compounds. The experimental geometries and spectroscopic measurements (IR, NMR) of the least and most oxidized compounds (**1** and **3**) were found in good agreement with B3LYP and MP2 results.

Experimental Section

General experimental procedure.

NMR data were recorded on a Bruker Avance III 400 MHz magnet operating at 400.21 MHz for ^{1}H and 100.64 MHz for ^{13}C. Chemical shifts are reported in ppm, *J* coupling constants in hertz (Hz) and the multiplicity of ^{1}H peaks are denoted with corresponding letters in italic (e.g., *s*: singlet, *d*: doublet, *dd*: doublet of doublets, *t*: triplet, *m*: multiplet, etc.). Ultra performance liquid chromatography experiments were accomplished with an Acquity UPLC, coupled to a Waters Synapt G2 QTOF mass spectrometer using an electrospray ionization (ESI) technique operating in positive or negative modes, and were performed with an Acquity UPLC BEH C18 1.7 µm 2.1 x 100 mm column from Waters. A linear gradient system was used for the UPLC separation, consisting of 1% formic acid in deionized water (Solvent A) and 1% formic acid in acetonitrile (solvent B) with a constant flow rate of 0.30 mL min^{-1}: 0 to 2 min (95%

A: 5% B), 2 to 30 min (1% A: 99% B), 30 to 40 min (1% A: 99% B), 40 to 45 min (95% A: 5% B), 45 to 60 min (95% A: 5% B). TOF MS data were acquired in the range of 100-1200 atomic mass units (amu) for a scan time of 0.5 seconds, using the electrospray positive mode (ES+). The cone voltage was ramped from 20 to 40 V. LC MS and MS/MS chromatograms were processed and visualized using the MassLynx v.4.1 software and further improved with CorelDraw X7. Thin layer chromatography was performed on Merck silica gel 60 F_{254} plates which were later visualized with either iodine or 254 and 366 nm UV lights; column chromatography was performed on Merck silica gel 60 (0.063-0.20 mm). X-ray diffraction experiments were realized on a Bruker D8 Venture diffractometer, using a Cu Kα source and a Photon 100 detector.

Drying, extraction and isolation.

Fresh African ginger rhizomes were received from the department of Enterprise Creation and Development (ECD) based at the Council for Scientific and Industrial Research (CSIR). The fresh rhizomes were harvested in Septembre 2014 from the cultivation site in Giyani, Limpopo Province, South Africa, and identified as *Siphonochilus aethiopicus* (Schweinf.) B.L. Burtt by ECD. 250g of fresh rhizomes were cut into 1-2 mm slices and portions were left to dry in a fume hood for approximately 11 days. The dried slices were subsequently grinded, and part of the resulting powder was stored in transparent plastic bags at room temperature for about nine months. Extracts for UPLC QTOF MS ES+ analysis were prepared by separately stirring overnight 10g of the crushed fresh rhizomes, powdered and processed plants and nine months stored powders in 100 ml of n-hexane/dicholoromethane (1:1) followed by filtration and evaporation of the solvent using a Büchi rotary evaporator. For the fresh rhizomes, the filtrate was concentrated with a rotary evaporator and dried out in a fume hood. Isolation of Siphonochilone (**1**) was done through silica gel column chromatography of the crude extract (0.565 g) prepared from the crushed fresh rhizomes. The extract was fractionated by gradient elution, starting with acetone/DCM (3:17) and progressively increasing up to acetone/DCM (2:3). A total of 21 fractions were collected, analyzed by TLC and grouped accordingly. TLC plates were developed with acetone/DCM (1:9) and alternately visualized with iodine and both 254 and 366 nm UV lights. 8 spots were revealed with the following R_f values 0.93, 0.86 (most intense spot), 0.78, 0.67, 0.58, 0.53, 0.22 and 0.16. Fractions 5 to 8, which displayed the most spot on the TLC plates, were combined and dried out to afford F1. F1 was resolved with silica gel column chromatography using an isocratic elution with EtOAc/n-hexane (3:17); and 80 sub-fractions were obtained. The sub-fractions were TLC analyzed using EtOAc/hexane (3:7), and the visualization of the plates was done using UV lamps and an iodine chamber. The sub-fractions 62 to 79 displayed a very intense spot with the R_f value of 0.68 and were accordingly mixed and concentrated with a Büchi rotary evaporator to afford F1a. Overnight crystallization of F1a gave Siphonochilone (**1)** as a colorless crystalline compound. Isolation of the lactone (**3**) was achieved in two steps using the n-hexane/dicholoromethane (1:1) extract (0.554 g) prepared from the stored powder. The first fractionation was done on a silica gel column using a gradient of acetone/DCM (from 3:17 to 2:3). 21 fractions were obtained and based on the TLC similarities, fractions 12-21 were mixed and the solvent evaporated. The combined fractions were further fractionated using silica gel column chromatography and an isocratic elution with the mixture acetone/EtOAc/n-hexane (2:3:5). A total of 80 sub-fractions were collected and analyzed by TLC using acetone/EtOAc/n-hexane (2:3:5). The plates were visualized with an iodine chamber. Based on TLC profiles, sub-fractions 12 to 37 were pooled and concentrated using a Büchi rotary evaporator, resulting in the lactone derivative **3** as colorless crystals.

Computational method

The initial geometries of **1** and **3** were built from the crystallographic data and optimized at B3LYP and MP2 theoretical levels, using 6-31+G(d,p) and 6-311+G(2d,p) basis sets. To ensure that the optimized geometries correspond to true minima on the potential energy surface, harmonic vibrational analysis was carried out at B3LYP/6-311+G(2d,p) level. The chemical shifts of **1** and **3** refer to C (182.4656) and H (31.8821) shielding of TMS and the 1H-H spin-spin coupling constants were computed, at B3LYP with 6-311+G(2d,p) in dichloromethane for **1** and chloroform for **3**, employing the polarizable continuum model (PCM). The optimized geometric structures and the spectroscopic data of **1** and **3** were compared with available experimental data. To predict reactivity of **1** and **3** frontier molecular orbitals were analyzed at MP2/6-31+G(d,p) because B3LYP has tendency to underestimate the HOMO-LUMO energy gap. All the calculations were obtained using Gaussian 09D.[(12)] For visualisation purpose ChemDraw, Gaussview5[(13)] and Chemcraft 4.3 were used.

Acknowledgements

The Department of Enterprise Creation (ECD) at the South African Council for Scientific and Industrial Research (CSIR) is acknowledged for the supply of African ginger rhizomes used for the present study. JT Muya thanks the Korea Research Fellowship program and grants from the Basic Science Research Program funded by the Ministry of Science, ICT and Future planning through the National Research Foundation of Korea (NRF2015H1D3A1062502) for support. FZJ Katele acknowledges BEBUC (Bourse d'Excellence Bringmann aux Universités Congolaises) and *f*UNIKIN (foerdeverein Uni Kinshasa e.V.) for the MSc scholarship, as well as and the Holger Pöhlmann Stiftung for support.

References

[1] R. Smith, *Bothalia* **1998**, *28*, 35-39.
[2] N. Crouch, M. Lotter,S. Krynauw, C. Pottas Bircher, *Herbertia* **2000**, *55*, 115-129.
[3] C.W. Holzapfel, W. Marais, P.L. Wessels, B. Van Wyk, *Phytochemistry* **2002**, *59*, 405-407.
[4] G. Fouche, S. Van Rooyen, T. Faleschini, *Int. J. Genuine Trad. Med.* **2013**, *3*, 24-29.
[5] C.A. Lategan, W.E. Campbell, T. Seaman, P.J. Smith, *J. Ethnopharmacol.* **2009**, *121*, 92-97.
[6] M. Light, L. McGaw, T. Rabe, S. Sparg, M. Taylor, D. Erasmus, A. Jäger, J. Van Staden, *S. Afr. J. Bot.* **2002**, *68*, 55-61.
[7] R.M Coopoosamy, K.K. Naidoo, L. Buwa, B. Mayekiso, *J. Med. Plant Res.* **2010**, *4*, 1228-1231.
[8] G. Fouche, N. Nieuwenhuizen, V. Maharaj, S. Van Rooyen, N. Harding, R. Nthambeleni, J. Jayakumar, F. Kirstein, B. Emedi, P. Meoni, *J. Ethnopharmacol.* **2011**, *133*, 843-849.
[9] a) C. Lee, W. Yang, R.G. Parr, *Phys. Rev. B* **1988**, *37* (2), 785-789; b) K.L. Schuchardt, B.T. Didier, T. Elsethagen, L. Sun, V. Gurumoorthi, J. Chase, J. Li, T.L. Windus, *J. Chem. Inf. Model.* **2007**, *47* (3), 1045-1052.
[10] F.P. Rotzinger, *J. Chem. Theory Comput*. **2009**, *5* (4), 1061-1067.
[11] M. Head-Gordon, J.A. Pople, M.J. Frish, *Chem. Phys. Lett.* **1988**, *153* (6), 503-506.
[12] M. J. Frisch, G. W. Trucks, H. B. Schlegel, G. E. Scuseria, M. A. Robb, J. R. Cheeseman, G. Scalmani, V. Barone, B. Mennucci, G. A. Petersson, H. Nakatsuji, M. Caricato, X. Li, H. P. Hratchian, A. F. Izmaylov, J. Bloino, G. Zheng, J. L. Sonnenberg, M. Hada, M. Ehara, K. Toyota, R. Fukuda, J. Hasegawa, M. Ishida, T. Nakajima, Y. Honda, O. Kitao, H. Nakai, T. Vreven, J. A. Montgomery, Jr., J. E. Peralta, F. Ogliaro, M. Bearpark, J. J. Heyd, E. Brothers, K. N. Kudin, V. N. Staroverov, R. Kobayashi, J. Normand, K. Raghavachari, A. Rendell, J. C. Burant, S. S. Iyengar, J. Tomasi, M. Cossi, N. Rega, J. M. Millam, M. Klene, J. E. Knox, J. B. Cross, V. Bakken, C. Adamo, J. Jaramillo, R. Gomperts, R. E. Stratmann, O. Yazyev, A. J. Austin, R. Cammi, C. Pomelli, J. W. Ochterski, R. L. Martin, K. Morokuma, V. G. Zakrzewski, G. A. Voth, P. Salvador, J. J. Dannenberg, S. Dapprich, A. D. Daniels, Ö. Farkas, J. B. Foresman, J. V. Ortiz, J. Cioslowski, and D. J. Fox, Gaussian 09, Revision D.01, Gaussian, Inc., Wallingford CT, 2009.
[13] R. Dennington, T. Keith, J. Millan, GaussView, version 5.0.8, Semichem Inc., Shawnee Mission KS, 2009.